Applied Catalysis, 12 (1984) 201–217
Elsevier Science Publishers B.V., Amsterdam — Printed in The Netherlands

CHARACTERIZATION OF Fe, Fe-Cu, AND Fe-Ag FISCHER-TROPSCH CATALYSTS

ISRAEL E. WACHS, DANIEL J. DWYER and ENRIQUE IGLESIA
Corporate Research Science Laboratories, Exxon Research and Engineering Company, Annandale, NJ 08801, U.S.A.

(Received 1 March 1984, accepted 7 August 1984)

ABSTRACT

Copper and silver were found to interact very differently with the oxidized iron catalyst. Copper is oxidized and highly dispersed on the passivated iron surface. The intimate contact between copper oxide and iron oxide and the facile reduction of copper oxide are responsible for the ability of copper to enhance the reduction of iron oxide. The metallic copper nuclei promote the nucleation stage of the iron oxide reduction process. Silver, unlike copper, is reduced and poorly dispersed on the passivated iron surface. This lack of intimate contact between silver and iron oxide prevents silver from enhancing the reduction of iron oxide. After reduction metallic copper and silver interact very similarly with the iron surface. Copper and silver are both agglomerated on the reduced iron surface. Copper and silver exhibit even less affinity for the carbided iron surface and additional agglomeration occurs when the Fe-IB catalysts are exposed to the H_2/CO reaction environment. The poor contact between the IB metals (copper and silver) and the iron surface in a H_2/CO reaction environment results in very similar product distributions during Fischer-Tropsch synthesis and rates of carbiding of the Fe-IB catalysts.

INTRODUCTION

Iron Fischer-Tropsch catalysts are usually prepared by precipitation, sintering, or melting of oxide mixtures [1]. The catalysts prepared by precipitation and sintering are used in fixed bed reactors at low temperature (220-280°C), and the fused catalysts are used in fluidized beds at higher temperatures (280-350°C). The relatively high activity of the precipitated and sintered catalysts allows their operation at lower temperature. These fixed bed catalysts are prepared with copper oxide in addition to the alkali and oxides typically present in iron Fischer-Tropsch catalysts. The addition of copper to an iron Fischer-Tropsch catalyst apparently enhances the rate of reduction and allows catalyst reduction at lower temperatures. The milder reduction conditions lead to iron Fischer-Tropsch catalysts possessing the high surface area required for active catalysts [1]. The presence of copper is also thought to favor the formation of iron carbide compounds during the H_2/CO reaction. The selectivity of the Fischer-Tropsch reaction, however, is apparently not affected by the presence of copper [1]. In order to understand the interaction between copper and iron in different reaction environments (O_2, H_2 and H_2/CO), in situ x-ray photoelectron spectroscopy

0166-9834/84/$03.00

(XPS), thermal gravimetric analysis (TGA), and X-ray diffraction (XRD) experiments were carried out. On-line gas chromatography allowed the analysis of the products during Fischer-Tropsch synthesis and the correlation of product distribution with the state of the catalyst surface. The study was also extended to silver-containing iron catalysts in order to determine differences that might exist between the iron-copper and the iron-silver systems.

EXPERIMENTAL

The experimental system has been described elsewhere [2]. It consists of a medium pressure micro-reactor coupled directly to a Leybold-Heraeus LHS-10 surface analysis system. The reactor and transfer device are similar in concept to that used by Bonzel and Krebs [3], but different in reactor design. Rather than rely on resistive heating of the catalyst, we have designed our reactor as a small volume (>10cc) gold-plated tube furnace. This design ensures that both the gas and sample are isothermal and that good gas mixing exists inside the reactor.

The iron-IB catalysts were prepared by impregnating Fe_2O_3 powder (Baker, 99.9% purity, ~8m^2/g) with $Cu(NO_3)_2 \cdot 2.5H_2O$ (Baker, 99.9% purity) and $AgNO_3$ (Baker and Adamson, 99.9% purity). The major impurity in the iron oxide powder was sulfur which was present as SO_4^{2-}. The impregnated catalysts were subsequently calcined at 500°C for 2 hours and reduced in flowing hydrogen at 500°C for 18.5 hours in order to intimately contact the IB metals with the iron catalyst. The reduced catalysts were passivated in a 2% O_2/He mixture prior to transfer to the micro-reactor. The atomic compositions of the reduced iron-IB catalysts were 1.40 and 1.35 percent copper and silver, respectively. The BET surface areas of the passivated Fe, Fe-Cu and Fe-Ag catalysts were 17, 14 and 6 m^2/g, respectively. Approximately 20 mg of the passivated material was pressed into a pellet and then mounted on a gold plated sample boat prior to inserting into the vacuum system. The sample boat could be manipulated from outside the vacuum system by magnetic motion feedthroughs. This system permits the removal of the sample from the reactor directly into the ultra-high vacuum system without exposure to air.

The H_2 and CO gases used in the study were purchased premixed from Scientific Gas in aluminum cylinders in order to reduce carbonyl formation. The high purity (99.99%) gas mixture was further purified by passing through a zeolite bed to remove water and through a copper bed to trap carbonyls. The gas pressure in the reactor was measured with a capacitance manometer and the flow regulated by a Tylan mass flow controller. Typical flow rates were 15 cm^3/min and the maximum CO conversion was ~1%. The reaction products were analyzed by a HP 5840 gas chromatograph (temperature programmed-chromosorb-102, FID and TCD detectors).

The iron X-ray photoelectron spectra were measured with a pass energy of 50 eV with an Al Kα excitation source. The copper and silver XPS spectra were measured with a pass energy of 100 eV. In order to minimize overlap between the Cu $2p_{3/2}$ XPS peak and the iron Auger peak, a Mg Kα excitation source was used to collect the copper XPS spectra. The spectrometer work function and high voltage amplifier were

calibrated by setting the binding energy of the Cu $2p_{3/2}$ at 932.8 eV and the Cu 3s at 122.9 eV.

Thermal gravimetric analysis (TGA) of the Fe-IB catalysts in H_2 (Linde, extra dry, 99.95%) and a 1:1 H_2/CO mixture (Matheson, 99.5%) were performed in a Mettler TA 2000C. A molecular sieve drier and Deoxo purifier scrubbed the gases prior to use. Seventy-five cm^3 (STP)/min of each gas were passed over 100 mg samples of catalyst. A temperature program of 12 °C/min to 500°C and isothermal at 500°C was adopted as a standard heating schedule.

X-ray powder diffraction patterns were obtained with a Philips diffractometer using Cu Kα radiation and a diffracted beam monochromator.

RESULTS

Bulk analysis of the reduced and passivated iron catalysts by x-ray diffraction showed the presence of α-Fe, a trace of Fe_3O_4, and some metallic Cu and Ag. Evidently a portion of the IB metals is agglomerated in the passivated catalysts.

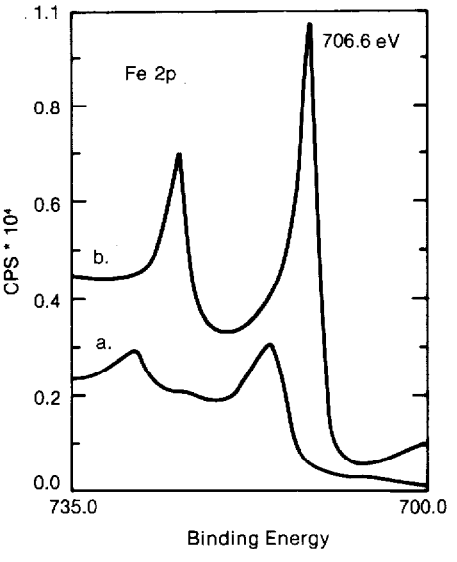

Figure 1 Fe $2p_{1/2,3/2}$ XPS spectra of iron catalyst a) passivated catalyst; b) after 1 hour reduction at 350°C.

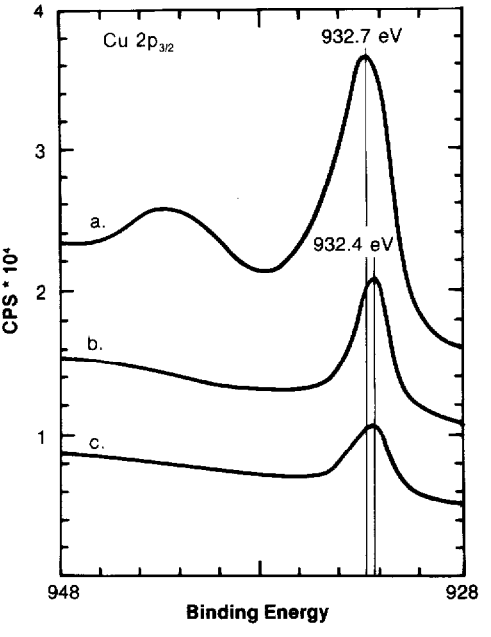

Figure 2 Cu $2p_{3/2}$ XPS spectra of Fe-Cu catalyst a) passivated catalyst; b) after 1 hour reduction at 350°C; c) after 16 hours reaction in H_2/CO environment.

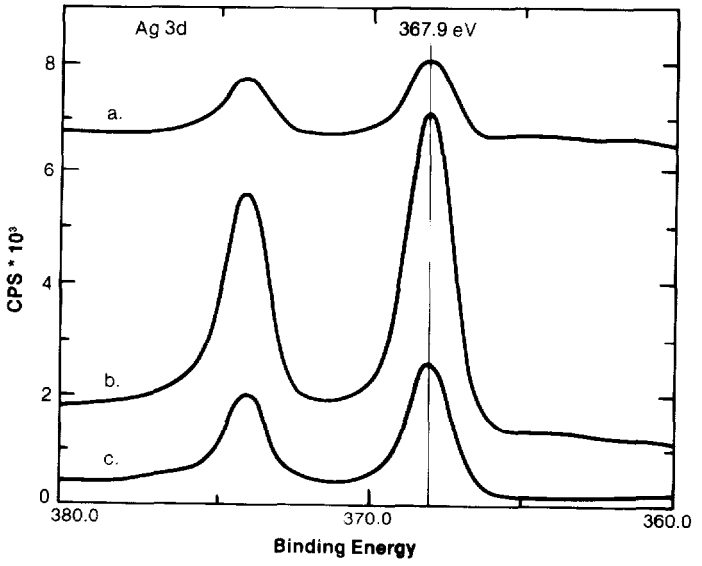

Figure 3 Ag $3d_{3/2,5/2}$ XPS spectra of Fe-Ag catalyst a) passivated catalyst; b) after 1 hour reduction at 350°C; c) after 16 hours reaction in H_2/CO environment.

No evidence for alloying between iron and the IB metals could be found in the diffraction patterns. However, low concentrations of IB metals in the iron catalyst would not cause detectable shifts in the iron diffraction peaks. Surface analysis of the passivated iron catalysts with XPS revealed that the iron surface is oxidized to Fe_2O_3. The XPS Fe $2p_{1/2,3/2}$ spectrum for the passivated iron sample is presented in Figure 1a. The Fe $2p_{3/2}$ binding energy of 710.9 eV and the iron oxide satellite peak at ~719 eV confirm that the surface iron is present as Fe_2O_3 [4,5]. The Cu $2p_{3/2}$ and the Ag $3d_{3/2,5/2}$ XPS spectra of the passivated catalysts are shown in Figures 2a and 3a, respectively. The Cu $2p_{3/2}$ XPS spectrum shows a satellite peak at ~943 eV, which is associated with CuO [4,6]. Not all the copper is oxidized to CuO since the ratio of the Cu $2p_{3/2}$ peak to the CuO satellite is 1.65 for CuO and is 3.9 for the passivated Fe-Cu catalyst and the binding energy of the Cu $2p_{3/2}$ XPS peak (932.7 eV) is between that for CuO (933.8 eV) and Cu_2O (932.5 eV) and Cu (932.4 eV). Only approximately 40% of the copper is estimated to be CuO; the rest of the copper is present as Cu_2O or Cu. It is not possible to distinguish between Cu_2O and metallic Cu because of the essentially identical binding energies of their Cu $2p_{3/2}$ peaks [4,6]. The Ag $3d_{5/2}$ XPS binding energy (367.9 eV) is consistent with the presence of metallic silver in the passivated Fe-Ag catalyst [4,7]. The oxide component of the silver XPS peak must be very small since the peak width does not change with reduction. The combined x-ray diffraction and XPS analysis of the

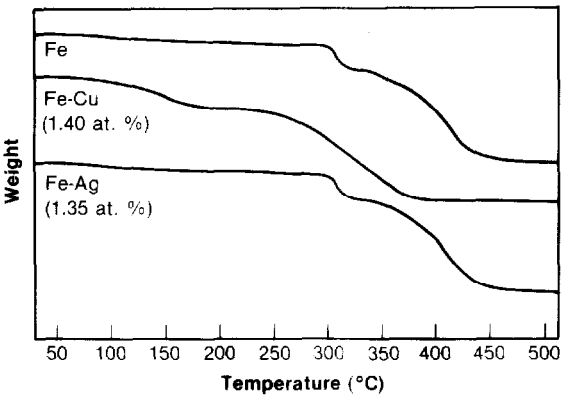

Figure 4 Reduction of passivated Fe-IB catalysts in hydrogen.

passivated iron catalysts demonstrates that the passivated catalysts consist of a metallic bulk and a very thin surface oxide layer.

The reduction of the passivated iron catalysts was examined in the TGA apparatus. The catalysts lost between 4-7% of their weight upon reduction. The loss of catalyst weight in flowing hydrogen as a function of temperature is presented in Figure 4. The reduction of the passivated iron catalyst starts at ~300°C and is complete at ~425°C. The passivated Fe-Ag catalyst exhibits a TGA spectrum identical to that of the passivated Fe sample. The TGA spectrum for the passivated Fe-Cu catalyst is, however, very different. Reduction of the passivated Fe-Cu catalyst is initiated at ~150°C and complete reduction is obtained at 370°C. The TGA experiments demonstrate that copper, but not silver, accelerates the reduction of oxidized iron.

The surface changes accompanying the reduction of the Fe-IB catalysts were monitored with XPS. The passivated Fe-IB catalysts were reduced in situ at 350°C for 1 hour in flowing hydrogen prior to the XPS analysis. The XPS scans of the surface of the iron catalyst before and after reduction are presented in Figure 5. After reduction the O 1s XPS signal was dramatically reduced and some sulfur and a trace of chlorine segregated to the iron surface. The carbon and sulfur occupied no more than 10% of the surface region (S, <2.5%; C, <7%). The XPS Fe $2p_{1/2,3/2}$, Cu $2p_{3/2}$, and Ag $3d_{3/2,5/2}$ spectra after reduction are presented in Figures 1b, 2b and 3b, respectively. The XPS binding energies of the Fe $2p_{3/2}$ (706.6 eV), Cu $2p_{3/2}$ (932.4 eV), and Ag $3d_{5/2}$ (367.9 eV) peaks are consistent with complete reduction of these elements to the metallic state [4-7]. After reduction, the intensity of the XPS Fe $2p_{1/2,3/2}$ signal increases because of the removal of the oxygen from the

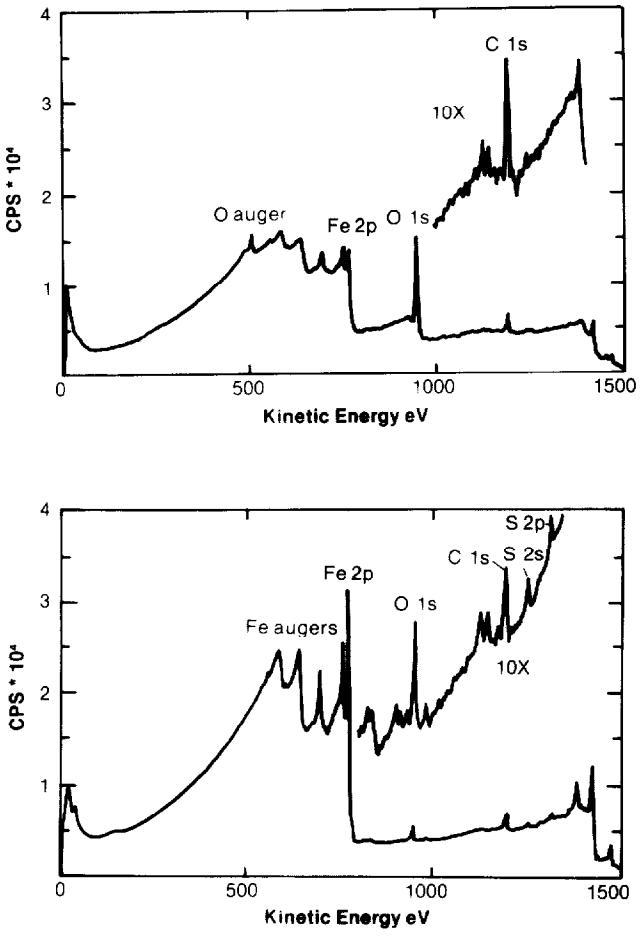

Figure 5 XPS survey scan of a) passivated iron catalyst; b) after 1 hour reduction of 350°C.

surface. The ratio of the Cu $2p_{3/2}$/Fe $2p_{1/2,3/2}$, Ag $3d_{5/2}$/Fe $2p_{1/2,3/2}$, and Cu $2p_{3/2}$/Ag $3d_{5/2}$ XPS signals are presented in Table 1. Note that relative to silver, copper is highly dispersed on the oxidized iron surface; however, after reduction, the two IB metals are comparably dispersed on the iron catalyst, with the copper XPS signal somewhat lower than the silver XPS signal. Upon reduction, the Ag/Fe XPS ratio increases, whereas the Cu/Fe XPS ratio decreases. The XPS data suggest that the Cu-Fe and Ag-Fe interactions are not identical.

The rates of carbon accumulation on the reduced iron catalysts in an H_2/CO environment were also examined with TGA. Figure 6 shows the rates of carbon

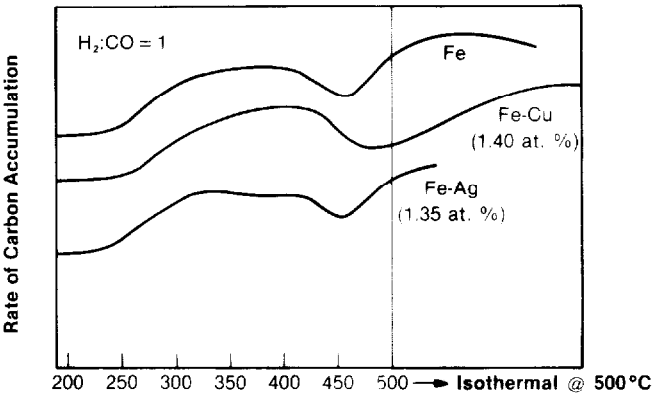

Figure 6 Rates of carbon accumulation of reduced Fe-IB catalysts in H_2/CO environment.

accumulation as a function of sample temperature. Two distinguishable stages of carbon accumulation are apparent: a low temperature stage, probably controlled by the diffusion of carbon into the iron bulk to form iron-Carbides, and a high temperature stage, controlled by the formation of coke or filamentous carbon . The rates of carbiding are essentially identical on the Fe, Fe-Cu, and Fe-Ag catalysts. However, the rates of coke/filamentous carbon production are only the same for Fe and Fe-Ag and somewhat slower for the Fe-Cu catalyst. X-ray diffraction of the carbon containing iron catalysts after the TGA experiments showed the presence of Fe_5C_2, a small amount of Fe_3C, and metallic Ag. The metallic Cu peak could not be observed due to overlap with the iron carbide diffraction peaks.

The surface changes occuring during H_2/CO catalysis over the Fe-IB catalysts were monitored in situ with XPS. The reaction conditions were 265°C, 7 atm and a H_2/CO ratio of 3. The changes in the Fe $2p_{1/2,3/2}$ and C 1s XPS spectra with extent of reaction are shown in Figures 7 and 8, respectively. The only significant change observed in the iron XPS spectra is an increase of ~0.3 eV (706.9 eV) in the binding energy of the Fe $2p_{3/2}$ peak. The carbon XPS spectra exhibit an increase in the carbon content after exposure of the reduced iron catalyst to the H_2/CO reaction environment and a decrease in the binding energy of the C 1s peak to 283.3 eV. The concomitant increase in the binding energy of Fe $2p_{3/2}$ and the appearance of a low binding energy form of carbon (283.3 eV) reflect the formation of an iron carbide phase [2,3]. A small amount of graphitic carbon is also deposited on the iron surface in the H_2/CO reaction environment; it gives rise to the shoulder on the high binding energy side of the XPS C 1s peak (see Figure 8) [2]. The amount of

graphitic carbon increases with reaction time. Essentially identical iron and carbon XPS results were obtained for the Fe-Cu and Fe-Ag catalysts. The XPS Cu $2p_{3/2}$ and Ag $3d_{3/2,5,2}$ spectra after 16 hours of reaction are presented in Figures

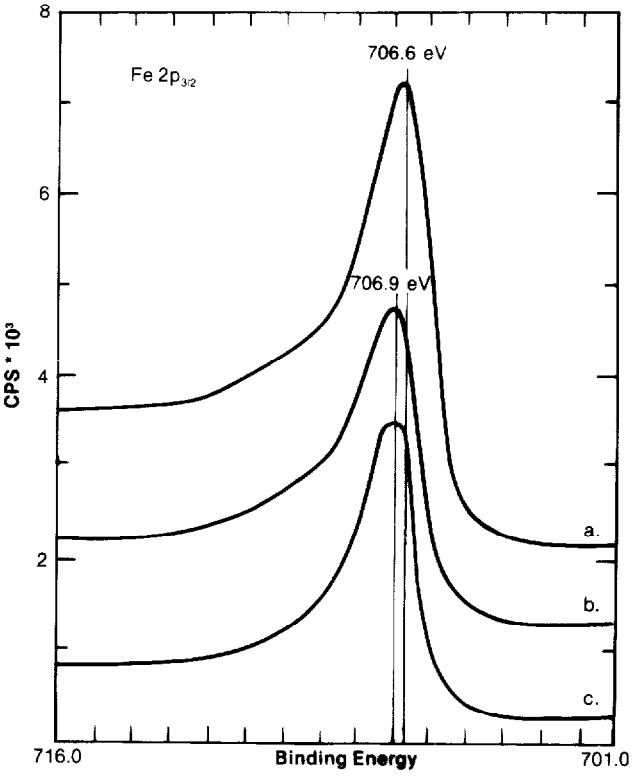

Figure 7 Fe $2p_{3/2}$ XPS spectra of iron catalyst a) after 1 hour reduction at 350°C; b) after 2 hours reaction in H_2/CO environment; c) after 16 hours reaction in H_2/CO environment.

2c and 3c, respectively. The XPS binding energies of Cu $2p_{3/2}$ (932.4 eV) and Ag $3d_{5/2}$ (367.9 eV) are not altered by the presence of carbon and are consistent with metallic copper and silver [4,6,7]. The Cu/Fe and Ag/Fe XPS ratios, however, decrease about 50% after exposure to the H_2/CO reaction environment, see Table 1. The greater escape depth of the Ag $3d_{5/2}$ XPS peak relative to the Fe $2p_{1/2,3/2}$ XPS peak ensures that the decrease in the Ag/Fe XPS ratio is not a consequence of the preferential attenuation of the silver XPS signal because of the accummulation of carbon on the catalyst surface. The Cu $2p_{3/2}$ XPS peak, however, has a shorter

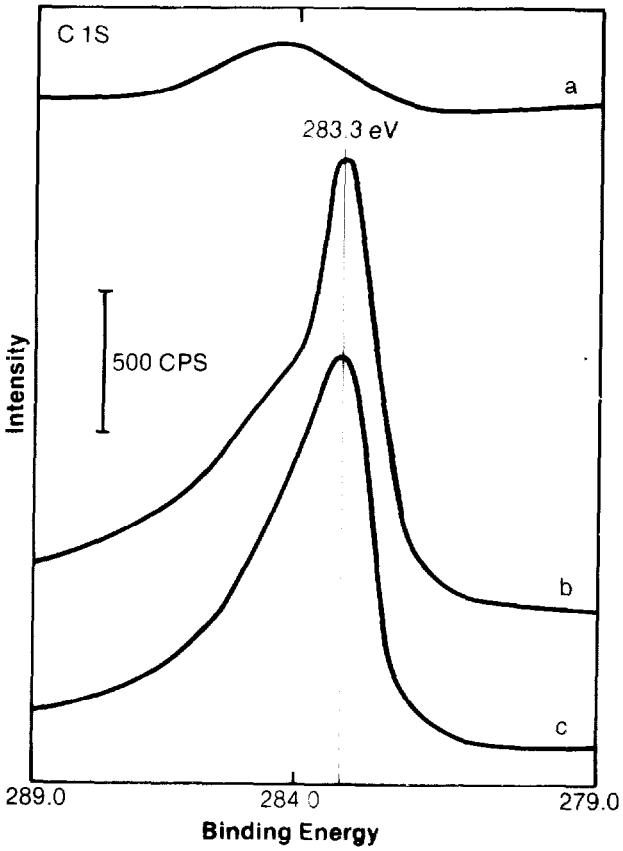

Figure 8 C 1s spectra of iron catalyst a) after 1 hour reduction at 350°C; b) after 2 hours reaction in H_2/CO environment; c) after 16 hours reaction in H_2/CO environment.

escape depth than the Fe $2p_{1/2,3/2}$ XPS peaks. To confirm that the decrease in the Cu/Fe XPS ratio is not caused by differences in the sampling depths, the x-ray induced Cu L_3VV Auger transition, which has an escape depth comparable to the Fe $2p_{1/2,3/2}$ transition, was also monitored. This peak also exhibits a comparable decrease in the Cu/Fe ratio with reaction. Thus, the copper and silver XPS signals from the iron surface decrease further in the H_2/CO reaction environment.

TABLE 1*

Treatment	Cu $2p_{3/2}$/Fe $2p_{1/2,3/2}$	Ag $3d_{5/2}$/Fe $2p_{1/2,3/2}$	Cu $2p_{3/2}$/Ag $3d_{5/2}$
Passivated	1.1	0.16	6.9
Reduced (350°C-1 hr)	0.16	0.22	0.73
H_2/CO (265°C-16 hr)	0.083	0.11	0.75

* Cu and Ag XPS spectra taken with a pass energy of 100 eV and Fe XPS spectrum taken with a pass energy of 50 eV. Cu, Ag, and Fe signals corrected for sensitivity factors[4], but not for different pass energies.

The product distribution from the H_2/CO reaction was monitored by on-line gas chromatography. The product distribution consisted predominantly of light paraffins, olefins and alcohols. Paraffins were the most abundant products, and methane was always the major reaction product on a mole basis. The behavior of the C_1 and C_2 products as a function of reaction time is presented for the iron catalyst in Figure 9. Note the initially low concentration of reaction products during the first few hours into the run prior to lining out of the catalyst.

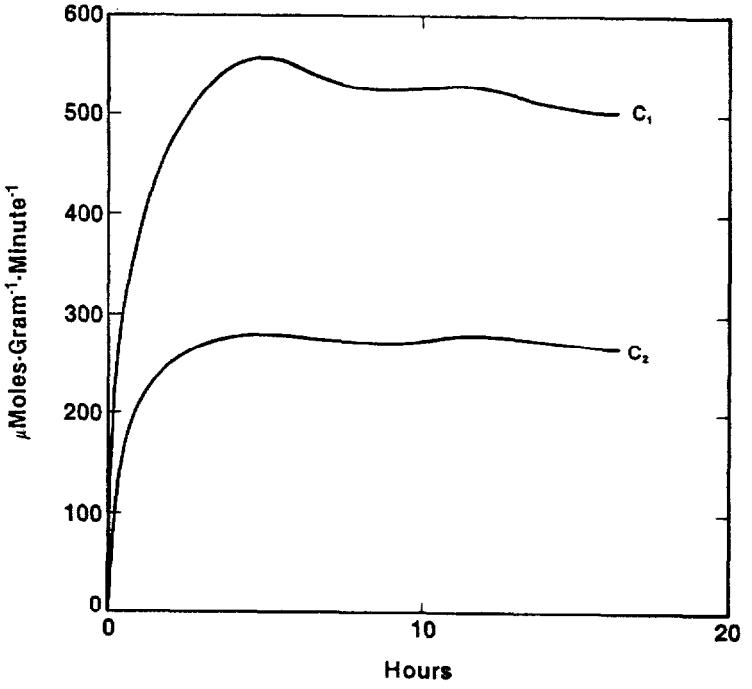

Figure 9 Transient behavior of C_1 and C_2 products during H_2/CO reaction for iron catalyst.

The product distribution for the iron catalyst is shown in Figure 10 at several different times into the run.

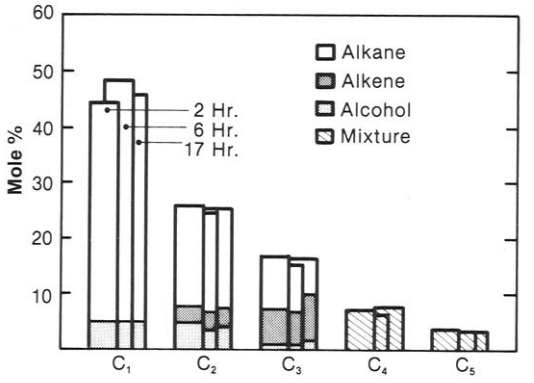

Figure 10 GC product distribution for iron catalyst during H_2/CO reaction.

After several hours on-stream the product distribution did not change appreciably. The same trend was observed for all the Fe-IB catalysts. The product distributions for the Fe-IB catalysts after 16 hours of reaction are compared in Figure 11.

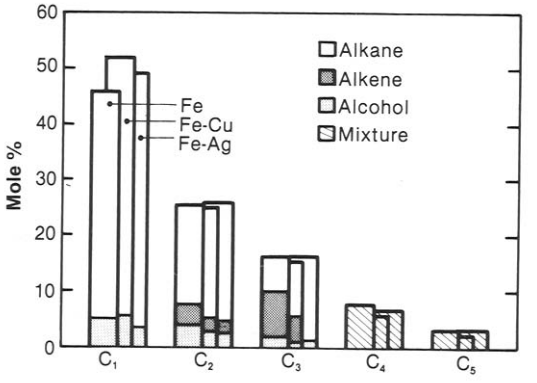

Figure 11 GC product distribution for Fe-IB catalysts after 16 hours of H_2/CO reaction.

Although some minor differences are observed in the product distributions of the Fe-IB catalysts, they are not significant. The Schulz-Flory α's for the Fe-IB catalysts are compared in Table 2; they are very similar for the three catalysts.

TABLE 2

Catalyst	Schulz-Flory α*
Fe	0.46 ± 0.01
Fe-Cu	0.45 ± 0.01
Fe-Ag	0.49 ± 0.01

*H_2/CO ratio = 3, ~265°C, 7 atm.

The Schulz-Flory α remained esentially constant after a few hours of reaction. The ethylene to ethane ratio, however, varied with reaction time and with the presence of IB metals. The ethylene/ethane ratio for the Fe-IB catalysts is shown in Figure 12 as a function of reaction time.

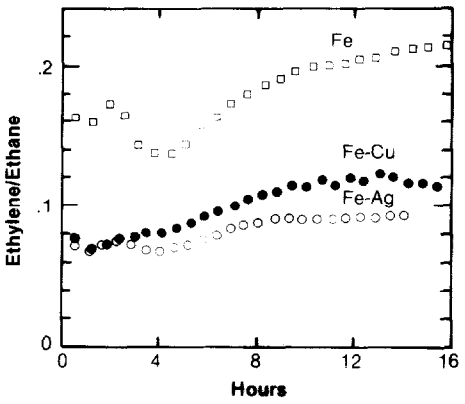

Figure 12 Transient behavior of ethylene/ethane ratio during H_2/CO reaction for Fe-IB catalysts.

After the initial transient, the ethylene/ethane ratios increase steadily throughout the runs and level off toward the last few hours of the runs. The small differences in the ethylene/ethane ratio for the Fe-IB catalysts are, however, much smaller than the order of magnitude changes in this ratio that result from the presence of potassium or graphite on the iron catalyst surface [2,3]. The addition of the IB metals to the iron catalyst does produce some changes in the products of the H_2/CO reaction, but these are minor. The reaction products are still predominantly paraffins, and methane accounts for approximately half of the hydrocarbon product on a molar basis.

DISCUSSION

The passivated iron catalyst consists of reduced iron containing a very thin oxide (Fe_2O_3) layer. The TGA reduction characteristics of this oxide layer are very similar to those of Fe_2O_3 [8]. Exposure of the reduced iron catalyst to the H_2/CO reaction environment results in carbiding of the bulk and surface of the catalyst. The XPS iron binding energy increases by ~0.3 eV due to the carbiding process. The predominant bulk carbide phase is Fe_5C_2 (Hagg carbide). Similar observations have been made in Mossbauer and magnetic susceptibility studies [9,10].

The product concentration from the H_2/CO reaction increases monotonically during the first few hours of the run and then levels off or declines slightly with reaction time. The initial low concentration of products in the gas-phase is a consequence of the depletion of the reactive surface carbon by diffusion of carbon into the iron bulk [11]. As this competitive pathway for carbon removal is retarded by the formation of bulk iron carbide, more surface carbon becomes available for the production of hydrocarbons. Magnetic susceptibility and Mossbauer studies have demonstrated that most of the bulk iron carbide is formed during the first few hours of reaction [9,10]. The reaction products are primarily paraffinic with methane being the predominant product. A very similar product distribution was obtained when this catalyst was examined in a Fischer-Tropsch fixed-bed reactor at high conversions of CO (97%) and high CO_2 selectivity (50%) [12]. The unpromoted iron catalyst formed predominantly light paraffins with C_1 accounting for ~50% of the hydrocarbon products on a mole basis. Thus, the product distribution obtained with the iron powder in the present reactor system is typical of an iron catalyst not promoted with alkali.

In this study, we have shown that Fe powders behave differently from reduced Fe foils in Fischer-Tropsch synthesis [2,3]. Iron foils give higher CH_4 selectivity than Fe powders (70 vs. 40 mol %); foils also deactivate extensively in a few hours because of the formation of a graphite carbon overlayer. In contrast, powders deactivate much more slowly and most of the carbon deposited in these samples is of a carbidic nature. The hydrocarbon chain growth probability is much larger on Fe powders (α = 0.46) than on foils (α = 0.3). The heavier product may result from the higher surface area and porosity of the powders, which lead to higher conversions than on Fe foils. The resulting higher H_2O and CO_2 concentrations, especially within catalyst pores, are probably responsible for the slower deactivation and the lower methane selectivity. We cannot rule out that the small amounts of surface sulfur on Fe powders are responsible for their different behavior. However, the very small surface sulfur concentrations (<3%), and the small reported effects of large amounts of sulfur on Fischer-Tropsch selectivity [15], lead us to prefer the alternate explanation.

Copper and silver interact very differently with the passivated iron catalyst. Copper is partially oxidized on the passivated iron surface and silver is

metallic. This trend is not unexpected because of the much higher heats of formation for the oxides of copper ($\Delta H°_f$=-37.5 kcal/mole for CuO and $\Delta H°_f$=-40.8 kcal/mole for Cu_2O) relative to the oxides of silver ($\Delta H°_f$=-6.3 kcal/mole for AgO and $\Delta H°_f$=-7.3 kcal/mole for Ag_2O). It is possible that the metallic silver surfaces or the oxidized copper surfaces are covered by an overlayer of iron oxide because of the much greater affinity of iron for oxygen ($\Delta H°_f$=-196.5 kcal/mole for Fe_2O_3, $\Delta H°_f$=-267 kcal/mole for Fe_3O_4 and $\Delta H°_f$=-64.3 kcal/mole for FeO). The oxidized copper is highly dispersed on the iron oxide surface whereas the metallic silver is poorly dispersed on the iron oxide surface. The metallic silver apparently has very little affinity for iron oxide and does not "wet" the oxidized iron surface, whereas the oxidized copper readily interacts with the oxidized iron surface.

The intimate contact between copper oxide and iron oxide is shown by the reduction behavior of the Fe-IB catalysts. The presence of copper in the passivated iron catalyst accelerates the reduction of the oxidized iron. According to the nucleation mechanism of oxide reduction, the reduction of oxides accelerates as the first metal nuclei are formed [13]. The lower reduction temperature of copper oxide (200-250°C) relative to iron oxide (~400°C) leads to the formation of metallic copper nuclei at temperatures where metallic iron ordinarily would not be formed. Thus, the promoting effect of copper oxide upon the reduction of iron oxide may be viewed as an increase in either the number of nucleation sites or the concentration of active hydrogen which is efficient in causing nucleation. Both of these processes result in promotion of the nucleation stage of reduction.

After reduction, metallic copper and silver interact very similarly with the iron surface. The surface concentrations of copper and silver on the reduced iron surface are similar. The dramatic decrease in the surface concentration of copper upon reduction of the iron surface may result from either agglomeration of copper or alloying between Cu and Fe. It is unlikely that the large decrease in the Cu XPS signal after reduction at 350°C results from alloying because alloying between copper and iron becomes significant only above 700°C [14]. Thus, the agglomeration of copper crystallites on the reduced iron surface must be responsible for the decrease in the surface concentration of copper. The surface concentration of silver on the iron surface increases somewhat after reduction; this may be a consequence of the loss in surface area of the Fe-Ag catalyst upon reduction. The solubility of silver in iron is extremely limited even at elevated temperatures [14], and alloying between silver and iron at 350°C is negligible. The surface concentrations of copper and silver on the iron surface decrease when the reduced Fe-IB catalysts are exposed to the H_2/CO reaction environment. Apparently, the IB metals have little affinity for the carbided iron surface and agglomerate further. The poor contact between the IB metals and the iron surface in a H_2/CO reaction environment accounts for the similar product distributions during Fischer-Tropsch synthesis and rates of carbon accumulation on the Fe-IB catalysts. Physical models

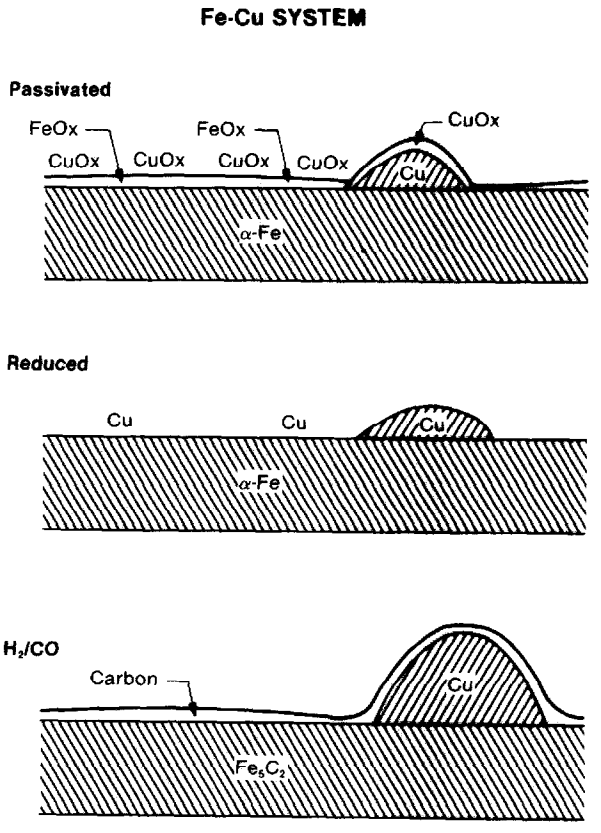

Figure 13 Model for behavior of the Fe-Cu system in oxidizing, reducing and H_2/CO reaction environments.

portraying the interactions between Fe-Cu and Fe-Ag in different environments (oxidizing, reducing, H_2/CO) are presented in Figures 13 and 14, respectively. These models are consistent with the data reported in this study. The present investigation demonstrates that the Fe-IB interactions are dynamic and are dependent on the reaction environment.

CONCLUSIONS

Copper and silver interact very differently with the oxidized iron catalyst. Copper is partially oxidized and highly dispersed on the passivated iron surface. The intimate contact between copper oxide and iron oxide and the facile reduction of copper oxide are responsible for the ability of copper to enhance the reduction of iron oxide. Silver, unlike copper, is reduced and poorly dispersed on the

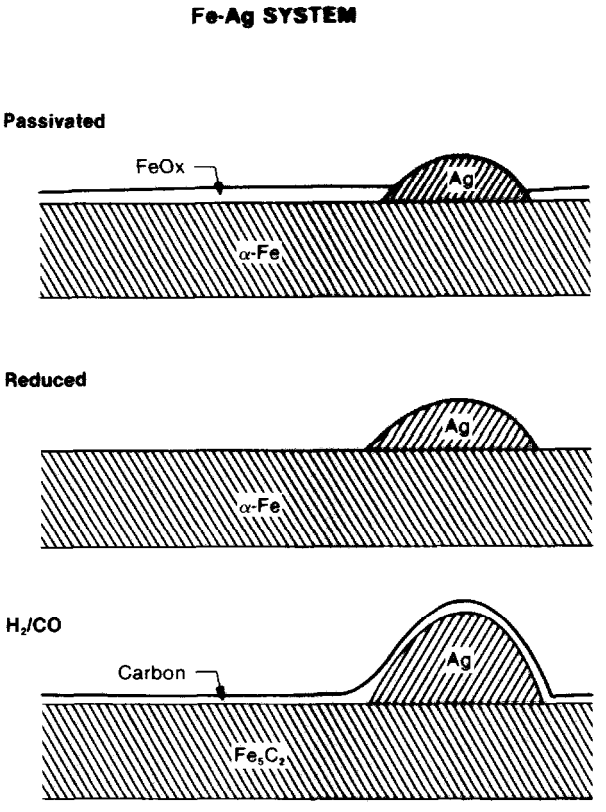

Figure 14 Model for behavior of the Fe-Ag system in oxidizing, reducing and H_2/CO reaction environments.

passivated iron surface. This lack of intimate contact between silver and iron oxide prevents silver from enhancing the reduction of iron oxide. After reduction metallic copper and silver interact very similarly with the iron surface. Copper and silver are both agglomerated on the reduced iron surface. Copper and silver exhibit even less affinity for the carbided iron surface and additional agglomeration occurs when the Fe-IB catalysts are exposed to the H_2/CO reaction environment. The poor contact between IB metals (copper and silver) and the iron surface in a H_2/CO reaction environment results in very similar product distributions during Fischer-Tropsch synthesis and rates of carbiding of the Fe-IB catalysts. The product distribution from the iron powder catalysts is primarily paraffinic, with methane accounting for approximately half of the reaction products on a mole basis. This product distribution is typical of an iron Fischer-Tropsch catalyst not promoted with alkali.

ACKNOWLEDGMENTS

The authors would like to thank John Hardenbergh for collecting the XPS data and S. Soled and B. DeRites for the TGA data.

REFERENCES

1 J. Falbe, Chemierohstoffe aus Kohle, chapter 8 (Fischer-Tropsch Synthesis), George Thieme Verlag, Stuttgart (1977).
M. E. Dry, "The Fischer-Tropsch Synthesis" in Catalysis Science and Technology, vol. 1, ed. by J. R. Anderson and M. Boudart, Springer-Verlag (1981).
2 D. J. Dwyer and J. H. Hardenberg, J. Catal. 87, 66 (1984).
3 H. P. Bonzel and H. J. Krebs, Surface Sci. 117, 639 (1982).
4 C. D. Wagner, M. W. Riggs, L. E. Davis, J. Moulder and G. E. Muilenberg, Handbook of X-ray and Photoelectron Spectroscopy, Physical Electronics Industries (1979).
5 K. Huokawa and M. Oku, Talanta 26, 855 (1979).
C. R. Brundle, T. J. Chuang and K. Wandelt, Surface Sci. 68 459 (1977).
S. R. Kelemen, A. Kaldor and D. J. Dwyer, Surface Sci. 121, 45 (1982).
6 T. H. Fleisch andG. J. Mains, Appl. Surface Sci. 10, 51 (1982).
7 J. S. Hammond, S. W. Gaarenstroom and N. Winograd, Analytical Chem. 47, 2193 (1975).
8 S. Soled, M. Richard, R. Fiato and B. DeRites, Thermal Analysis, Proc. 7th Inter. Conf. Thermal Analysis, p.1249 (1982).
9 (a) J. W. Niemantsverdriet, A. M. van der Kraan, W. L. Van Dijk, H. S. van der Baan, J. Phys. Chem. 84, 3363 (1980).
(b) J. A. Amelse, G. Grynkewich, J. B. Butt and L. H. Schwartz, J. Phys. Chem. 85, 2484 (1981).
(c) G. B. Raupp and W. N. Delgass, J. Catal. 58, 337 (1979).
(d) G. B. Raupp and W. N. Delgass, J. Catal. 58, 348 (1979).
(e) G. B. Raupp and W. N. Delgass, J. Catal. 58, 361 (1979).
10 K. M. Sancier, W. E. Isakson and H. Wise in Hydrocarbon Synthesis from Carbon Monoxide and Hydrogen, ed. by E. L. Kugler and F. W. Steffgen, Advances in Chemistry Series 178, American Chemical Society, (1979).
11 W. L. Van Dijk and H. S. Van der Baan, J. Catal. 78, 24 (1982).
12 M. A. Richard, J. C. Pirkle, Jr., and F. J. Wright, Eighth North American Catalysis Society Meeting, Philadelphia, May 1983.
13 N. W. Hurst, S. J. Gentry, A. Jones and B. O. McNicols, Catal. Rev. Sci. Eng. 24, 233 (1982).
14 M. Hansen, Constitution of Binary Alloys, McGraw-Hill, New York (1958).
15 R. J. Madon and H. Shaw, Catal. Rev. Sci. Eng., 15(1), 69 (1977).